

1986

Computer Modeling of Scroll Compressor with Self Adjusting Back-Pressure Mechanism

K. Tojo

M. Ikegawa

N. Maeda

S. Machida

M. Shilbayashi

See next page for additional authors

Follow this and additional works at: <https://docs.lib.purdue.edu/icec>

Tojo, K.; Ikegawa, M.; Maeda, N.; Machida, S.; Shilbayashi, M.; and Uchikawa, N., "Computer Modeling of Scroll Compressor with Self Adjusting Back-Pressure Mechanism" (1986). *International Compressor Engineering Conference*. Paper 576.
<https://docs.lib.purdue.edu/icec/576>

This document has been made available through Purdue e-Pubs, a service of the Purdue University Libraries. Please contact epubs@purdue.edu for additional information.

Complete proceedings may be acquired in print and on CD-ROM directly from the Ray W. Herrick Laboratories at <https://engineering.purdue.edu/Herrick/Events/orderlit.html>

Authors

K. Tojo, M. Ikegawa, N. Maeda, S. Machida, M. Shilbayashi, and N. Uchikawa

COMPUTER MODELING OF SCROLL COMPRESSOR
WITH SELF ADJUSTING BACK-PRESSURE MECHANISM

Kenji TOJO, Masato IKEGAWA, Naoki MAEDA, Sigeru MACHIDA,
Masao SHIIBAYASHI
Mechanical Engineering Research Laboratory, Hitachi Ltd.
Tsuchiura, Ibaraki, Japan

Naoshi Uchikawa
Shimizu Works, Hitachi Ltd.
Shimizu, Shizuoka, Japan

ABSTRACT

A computer model for calculating the performance of a scroll compressor with a self-adjusting back-pressure mechanism was developed. The model gives detailed geometrical and thermodynamic information concerning the internal processes. It calculates the influence of internal leakage between the neighboring gas pockets with its viscous effect. It also calculates the contribution to adiabatic inefficiency from gas flow passing through small apertures located in positions opened to the intermediate compression gas pockets.

This paper describes the theory used in the model and then presents some numerical results of p-v diagram, back-pressure, and the adiabatic efficiency of the machine for several operating conditions.

INTRODUCTION

With the popularization of air-cooled and heat-pump air conditioners, the energy efficiency ratio and high compressor efficiency over a wide range of operating conditions must be improved. Likewise, to improve the annual performance factor of heat-pump air conditioners, capacity control by means of motor rotational speed control is becoming widespread. Low noise/vibration level at all rotational speeds is another important consideration for compressors. With this in mind, a new type of compressor with scroll wraps was developed and put into commercial production⁵⁾. The concept of a scroll fluid machine is very old. It was first described in a U.S. patent in the early 1900s¹⁾, but was not fully developed in the practical application until recently^{2,3)}. This was primarily because of the lack of precise production techniques and the component wear resulting from the large axial

gas force. To solve these problems, Hitachi developed a precise machining technique for mass production, and also developed a controlled thrust force mechanism to support the orbiting scroll in the axial direction with the lowest frictional force and wear⁴). In the controlled thrust force mechanism, so-called a back-pressure chamber is provided behind the orbiting scroll. The back-pressure chamber is pressurized automatically at a level between the suction pressure and the discharge pressure by means of gas introduced through the small apertures (back-pressure port) open to the intermediate compression gas pockets, and provide pneumatic force against the back of the orbiting scroll.

While a calculative method to find the proper range of the back-pressure on the back of the orbiting scroll has been reported⁶), it is necessary to investigate the dynamic characteristics involved as well. Thus, this paper outlines a computer simulation model for analyzing the performance of a scroll compressor with a self adjusting back-pressure mechanism. The model gives detailed geometrical and thermodynamic information to the compression gas pockets and to the back pressure chamber. Application of this is demonstrated by an actual example of the scroll wraps.

GEOMETRICAL CHARACTERISTICS

The main elements in a scroll compressor are two identical involute spiral scrolls shown in Fig.1. They are assembled at a relative angle of 180° so that they touch at several points and form a series of crescent-shaped pockets. One of the scroll member is fixed and the other orbits around the center of the fixed scroll wrap. The orbiting scroll is driven by a fixed short-throw crank mechanism. The pair of contact points between the two spiral walls shift along the spiral curves with shaft rotation. The relative angle of the two scroll members are maintained by means of an anti-rotation coupling mechanism located between the back of the orbiting scroll plate and the stationary part.

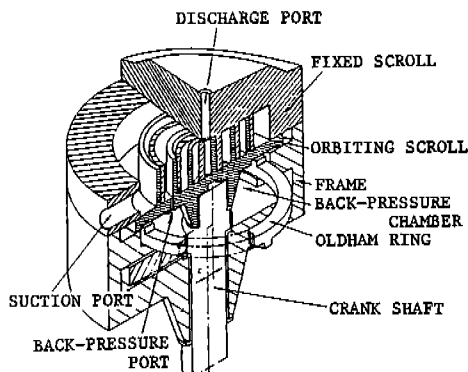


Figure 1 Basic configuration of scroll compressor

Volume curve

The geometrical relation of scroll wrap is shown in Fig.2, and 3. When the n pairs of pockets are formed, as shown in Fig.3, the roll angles, λ_{pi} at the contact points are given as:

$$\begin{aligned} \lambda_{pi} &= \left(-\theta + \frac{1}{2}\pi\right) + 2(i-1)\pi & 0 \leq \theta \leq \frac{1}{2}\pi \\ &= \left(-\theta + \frac{1}{2}\pi\right) + 2i\pi & \frac{1}{2}\pi \leq \theta \leq 2\pi \end{aligned} \quad (1)$$

The volume of the i -th pocket, V_{pi} , is obtained from the geometrical consideration of the involute spiral as follows;

$$V_{pi} = \alpha \pi a h^2 [2 (\lambda_{pi} - \pi) + \alpha] \quad (2)$$

The displacement volume, V_{th} , and the built in volume-ratio, V_r , are then given as:

$$V_{th} = \alpha \pi a h^2 [2 (\lambda_{ps0} - \pi) + \alpha] \quad (3)$$

$$V_r = \frac{2 (\lambda_{ps0} - \pi) + \alpha}{2 (\lambda_{pdo} - \pi) + \alpha} \quad (4)$$

where λ_{ps0} is the roll angle at the seal-off position of the suction pockets, and λ_{pdo} is the roll angle at the contact point when the discharge process commences.

The volume of the outermost pocket in the suction process illustrated by the shaded area in Figure 3 is given as:

$$\begin{aligned} V_{pi} &= \alpha a^2 h \left[\frac{1}{2} \theta_s (2\lambda_{ps0} - \theta_s + \alpha) \right. \\ &\quad \left. + \lambda_{ps0} \sin \theta_s + \frac{1}{4} \alpha \sin 2\theta_s - (1 - \cos \theta_s) \right] \end{aligned} \quad (5)$$

where θ_s is the orbiting angle taken from the suction seal off position.

The innermost sealed pocket in the discharge process is defined by the dotted area in Fig.3. The volume of the pocket in the discharge process is given as:

$$V_{pi} = h \left[\frac{1}{6} a^2 \{ (\lambda_{pl} + \pi)^3 - \lambda_{pl}^3 \} + a^2 (\pi - 2\alpha) \right]$$

$$\begin{aligned}
& - \frac{1}{6} a^2 \{ (\lambda_{p1} + \pi)^3 - (\lambda_{pdo} - 2\pi)^3 - (\lambda_{p1} + \alpha)^3 + (\lambda_{pdo} - 2\pi + \alpha)^3 \} \\
& - \left\{ \frac{1}{2} r_c^2 \left(\frac{1}{2} \pi + \phi \right) + a r_c \sin \phi + 2a \left(a \left(\lambda_{pdo} - 2\pi + \alpha \right) + r_c \right) + \frac{1}{2} \pi a^2 \right\} \\
& - S_0] \tag{6}
\end{aligned}$$

where $\phi = \cos^{-1}(2a/r_c)$, and S_0 is defined by the shaded area in Fig.4.

The volume curve calculated for sample scroll wraps is shown in Fig.5. The pocket in the suction process reaches its maximum volume slightly before the suction pocket seals off. In the compression process, the sealed pocket decreases its volume at a constant rate as the contact point moves toward the center of the spiral. At the end of the discharge process, a small amount of volume remains in the innermost sealed pocket.

Sealing line length

Since the pressures of a pair of compression pockets are assumed to be identical, the sealing line for radial leakage flow at the tip of scroll wrap is defined as follows.

compression process

$$L_{agi} = \frac{1}{2} a [(\lambda_{pi} + \alpha)^2 - (\lambda_{pi} - \beta)^2] \tag{7}$$

suction process

$$\begin{aligned}
L_{agi} &= \frac{1}{2} a [(\lambda_{pso} + \alpha)^2 - (\lambda_{pi} - \alpha)^2] & 0 \leq \theta_s \leq \pi \\
&= \frac{1}{2} a [(\lambda_{pso} + \alpha)^2 - (\lambda_{pso} - \beta)^2] & \pi \leq \theta_s \leq 2\pi \tag{8}
\end{aligned}$$

The sealing line for tangential leakage flow at the flank of the scroll wrap is represented by the wrap height.

Suction and discharge flow area

When the involute of the scroll wrap is machined by a cutter whose diameter is equal to the width of the scroll groove, the discharge roll angle is determined by the interaction between the involute spiral and the cutter. As shown in Fig.4, the inner line between P and Q is an arc with the same radius as that of the cutter. Therefore, the discharge flow area is formed between the pointed end of the scroll wrap and the inner wall of the scroll wrap as described above. Then it is given by:

$$A_{gd} = h \left[r_c - \sqrt{\epsilon^2 + (r_c - \epsilon)^2 - 2\epsilon(r_c - \epsilon) \cos(\pi - \theta_d)} \right] \quad (9)$$

The suction flow area is determined from the scroll wrap geometry shown in Fig.3 as follows.

$$A_{gs} = h\epsilon (1 - \cos \theta_s) \quad (10)$$

The sealing line length and the suction and discharge flow area for sample scroll wrap characterized in Table 1 are shown in Fig.5. The leakage path area is obtained as the product of the line length and the clearance.

ANALYTICAL MODEL

The working space of the scroll compressor is modeled by plural compression pockets, the suction chamber, the discharge chamber, and the back-pressure chamber. The latter is connected to the intermediate compression chamber through the small apertures on the orbiting scroll, as shown in Fig.7.

The pressure in the back-pressure chamber is adjusted automatically by means of gas introduced through the the small apertures, and provides an axial pneumatic force against the back of the orbiting scroll to support it in the axial direction. Therefore, the effect of internal leakage between the neighboring pockets and also the effect of gas drawing in and out were considered. In order to simplify the calculations, the following assumption were made.

- 1) The properties of the working fluid is homogeneous throughout the working space at any instant.
- 2) The working fluid is treated as an ideal gas with a constant specific heat.
- 3) Gravitational and kinematic energies of the working fluid are neglected.

From the First Law of Thermodynamics and the Law of Conservation of Mass, the following fundamental equations were obtained.

$$\frac{dT}{d\tau} = T \left[\frac{1}{G} \left(\kappa \frac{T_{gi}}{T} - 1 \right) \frac{dG_{gi}}{d\tau} - \frac{1}{G} (\kappa - 1) \frac{dG_{go}}{d\tau} - \frac{(\kappa - 1)}{V} \frac{dV}{d\tau} + \frac{A_w H_w}{C_p G} \left(\frac{T_w}{T} - 1 \right) \right] \quad (11)$$

$$\frac{dP}{d\tau} = P \left[\frac{\kappa}{G} \frac{T_{gi}}{T} \frac{dG_{gi}}{d\tau} - \frac{\kappa}{G} \frac{dG_{go}}{d\tau} - \frac{\kappa}{V} \frac{dV}{d\tau} + \frac{A_w H_w}{C_p G} \left(\frac{T_w}{T} - 1 \right) \right] \quad (12)$$

$$\frac{dG}{d\tau} = \frac{dG_{gi}}{d\tau} - \frac{dG_{go}}{d\tau} \quad (13)$$

By use of these equations, change in the state of the working fluid can be calculated in a step-by-step procedure.

Back-pressure chamber

The same principle as mentioned above was applied to consider a change in state of the working fluid in the back pressure-chamber. However, in this case, the volume of the back-pressure chamber is constant.

Suction and discharge process

The equations obtained above were also used for analysis of the suction and discharge processes. For the sake of simplicity, the suction and discharge chamber pressure were assumed to be constant.

Leakage flow rate

In the scroll compressor, leakage from the higher to the lower pressure pockets through the positive clearances between the flanks of the wraps (radial clearance) and between the tip of the wrap and the end plate (axial clearance) is the largest factor governing both the volumetric and the adiabatic efficiencies. The leakage paths as shown in Fig.8, are narrow and long compared with their height. Thus, the viscous effect should be taken into account in leakage analysis. The leakage path is modeled by the two dimensional flow channel which consists of the high pressure chamber, a convergent nozzle, a straight channel including the viscous drag and the low pressure chamber. The straight channel has a constant rectangular cross section. The length of the straight channel is specified so that the frictional loss in the model channel is equivalent to that in the practical leakage path. The mass flow rate in the channel is calculated as the adiabatic flow with fluid friction (Fanno flow)⁹).

Flow through back-pressure port

The small amount of gas drawing in and out through the back pressure ports that opened to the intermediate compression pockets has an effect on the adiabatic efficiency and the pressure level in the back pressure chamber. The flow rate passing through the back pressure ports is obtained using well-known equation of flow through a convergent-divergent nozzle.

OUTLINE OF COMPUTER PROGRAM

The flow diagram of the computer program is shown in Fig.8. The program requires physical characteristics of the compressor and the operating parameters as input. The calculation of properties starts from the suction process with an assumed temperature and pressure in the sealed pockets and the back pressure chamber. The initial properties in the intermediate compression pockets are calculated under the condition of no leakage. In the back pressure chamber it is assumed the values are average for the sealed pockets which open to the back pressure ports. The mass flow rate and the properties of the working fluid are

calculated at a small integration step using the Runge-Kutta method. After completion of each cycle, the adiabatic efficiency is calculated and compared with calculation for the previous cycle. This calculation is iterated until the system converges. Finally, the properties of the working fluid at every orbiting angle, P-V diagram, volumetric efficiency, etc. are obtained.

RESULTS AND DISCUSSION

Influence of clearances

The P-V diagram and the variation of efficiency in the case of several axial and radial clearances are shown in Fig.9, 10 and 11. The P-V diagram shows that the increase of axial clearance causes a comparatively small bulge of pressure in the first half of the compression process, whereas the increase of radial clearance causes a large rise in pressure in the latter half of the compression process.

The reason for this is as follows. The axial clearance increases the gas leakage in the peripheral region of the scroll wraps and influences the volumetric efficiency since the axial sealing line length increases proportionally to the roll angle of the scroll wrap, as was shown in Figure 6. On the other hand, the radial clearance increases the gas leakage in the center region of the wraps because their parts have shorter radii of curvature. This reduces the equivalent length of the leakage flow paths and the frictional loss, and the difference in pressure between the neighboring compression gas pockets is large.

This would mean that the gas leakage through the clearance of scroll wrap is dominated by the gas passing through the radial clearance in the center region of the scroll wraps and by that passing through the axial clearance in the peripheral region of the scroll wraps.

Influence of back pressure chamber

The back pressure-chamber is connected with the intermediate compression pockets during the compression process via the back-pressure ports. The diameter of the back-pressure ports and the volume of the back-pressure chamber influence not only the pressure rise of the P-V diagram but also the pressure level in the back-pressure chamber.

The influence of the back-pressure ports diameter size on the pressure change in compression pockets and in the back-pressure chamber is shown in Fig.12. As shown in this figure, a small amount of gas drawing in and out through the back-pressure port expands the pressure line outward during the compression process when the gas pocket opens to the back-pressure port, and results in compression power loss.

The effect of the back-pressure ports area on the adiabatic efficiency and the average back-pressure level is shown in Fig.13. In this figure, the adiabatic efficiency of the compressor without a back-pressure chamber was taken as 100%.

As is evident from these figures, the larger the effective flow-

passage area of the back-pressure ports is, the larger the pressure rise in the P-V diagram, the lower the adiabatic efficiency, and the higher the pressure level in the back-pressure chamber are. Since the effective flow passage area at the back pressure ports under practical operating conditions is considerably small, the resulting efficiency reduction is negligible, and little pressure fluctuation in the back-pressure chamber is observed. Thus the mechanism to obtain the pressure in the back pressure chamber through back-pressure ports adjusts the axial gas force against the back of the orbiting scroll to the proper range automatically wherever there is a change in operating conditions.

CONCLUSIONS

A computer model for evaluating the performance of a scroll compressor with a back-pressure chamber was developed. The model includes calculation of compressor's geometrical figure, and analysis of the working fluid properties in the sealed pockets. In this analysis, the influence of internal leakage between the neighboring pockets with viscous effect and the influence of the back-pressure chamber connected to the intermediate compression pockets through the small apertures were considered. The result of calculation on sample scroll wraps proved the following:

- 1) In the center region of scroll wraps, the leakage through the radial clearance is dominant and has considerable influences on the adiabatic efficiency.
- 2) In the peripheral region of wraps, the leakage through axial clearance is dominant and influences the volumetric efficiency.
- 3) The enlargement of effective flow area at the back-pressure ports reduces the adiabatic efficiency and enhances the pressure level in the back-pressure chamber.

NOMENCLATURE

a	= radius of basic circle of the involute spiral
A_{gd}	= discharge flow area
A_{gs}	= suction flow area
C_v	= specific heat at constant volume
G_{gi}	= mass flow into the sealed pocket
G_{go}	= mass flow out of the sealed pocket
G	= mass of the gas in the sealed pocket
h	= wrap height
L_{agi}	= seal line length at the top of the wrap
L_{gri}	= seal line length at the flank of the wrap
r_c	= radius of the cutter
T	= temperature
P	= pressure
P_s	= suction pressure
P_d	= discharge pressure
t	= wrap thickness
V_b	= back-pressure chamber volume

V_{pi} = sealed pocket volume
 V_{th} = displacement volume
 V_r = built-in volume ratio
 λ_{pi} = roll angle of the involute spiral
 λ_{ps0} = roll angle at the suction seal-off position
 λ_{pdc} = roll angle at the discharge starting position
 ϵ = orbiting radius
 θ = orbiting angle
 κ = specific heat ratio
 α = ϵ/a
 β = t/a

REFERENCES

- 1) L. Creux, "Rotary Engine" U.S. Patent No.801182, 1905.
- 2) R.W. Moore, Jr., et al, "A Scroll Compressor for Shipboard Helium Liquefier System", Proc. of the 1976 Purdue Compressor Technology Conference.
- 3) J. E. McCullogh, et al, "The Scroll Machine - An Old Principle with a New Twist", Mechanical Engineering , Vol.101, No.12, 1979.
- 4) E. Sato, "Scroll Compressor", U.S.Patent NO. 4475874.
- 5) Journal of the Japan Society of Mechanical Engineers, Vol.86, No.776, 1983, p433.
- 6) M.Ikegawa, et al, "Scroll Compressor with Self-Adjusting Back pressure Mechanism", ASHRAE Transactions, vol.90, Pt.2, No.2846, 1984.
- 7) K. Tojo, et al, "A Scroll Compressor for Air Conditioners", Proc. of the 1984 Purdue Compressor Technology Conference.
- 8) N,Arai, et al, "Scroll and Screw Compressors : The Latest Compressor Technology for Air Conditioning and Refrigeration", Hitachi Review Vol.34, No.3, 1985.
- 9) JSME DATA BOOK "Hydraulic Losses in Pipe and Ducts", JSME Japan, 1980.
- 10) T. YANAGISAWA, et al, "Leakage Losses with a rolling piston type rotary compressor", Refrigeration, Vol.8, No.2, 1985.

Table 1 Scroll compressor specifications

Displacement volume	V_{th}	cc/rev	75.0
Built-in volume ratio	V_r		2.7
Basic circle radius	a	mm	2.6
Orbiting radius	ϵ	mm	4.5
Wrap thickness	t	mm	3.6
Wrap height	h	mm	37.6

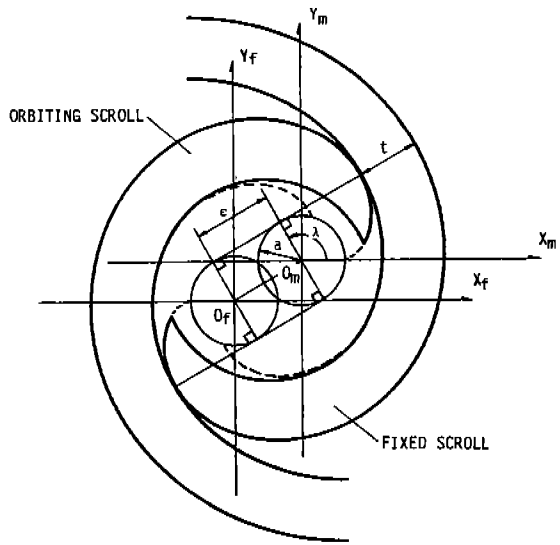


Figure 2 Geometrical relation of scroll wrap

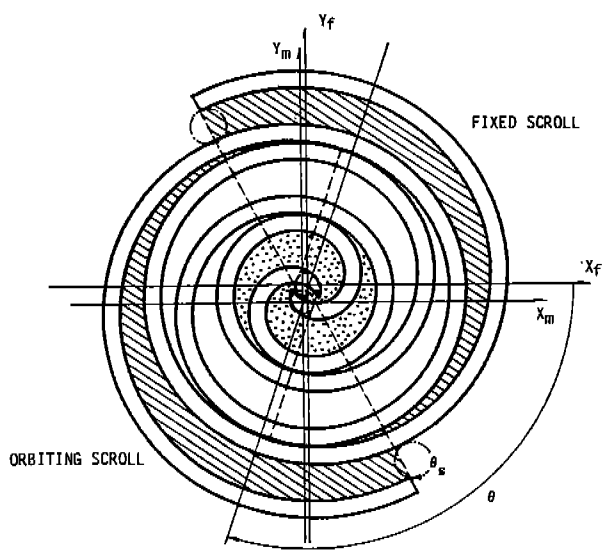


Figure 3 Sealed gas pocket of scroll compressor

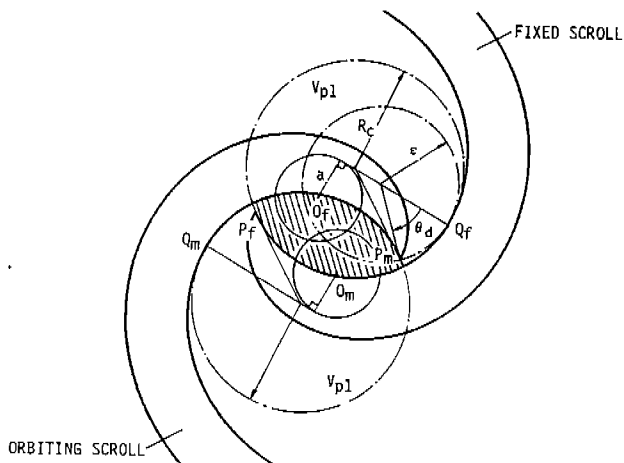


Figure 4 Innermost sealed pocket and discharge flow area

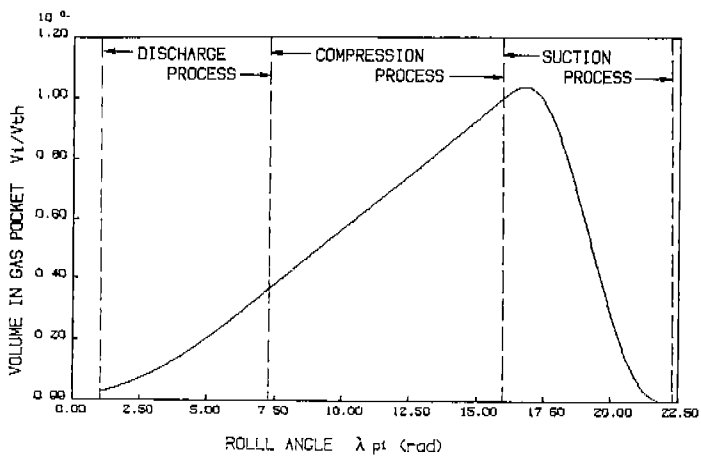


Figure 5 Volume curve of scroll compressor

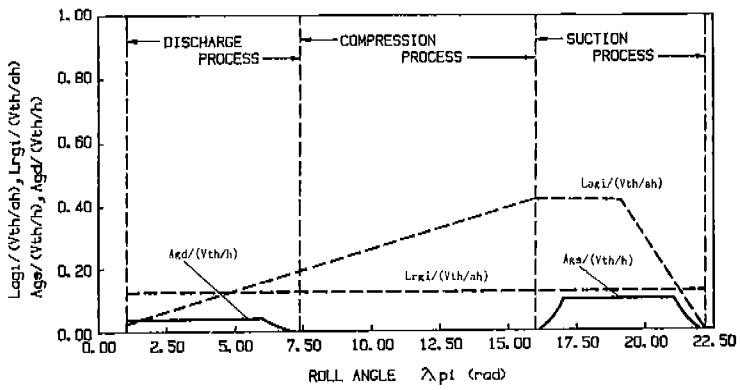


Figure 6 Suction and discharge flow area

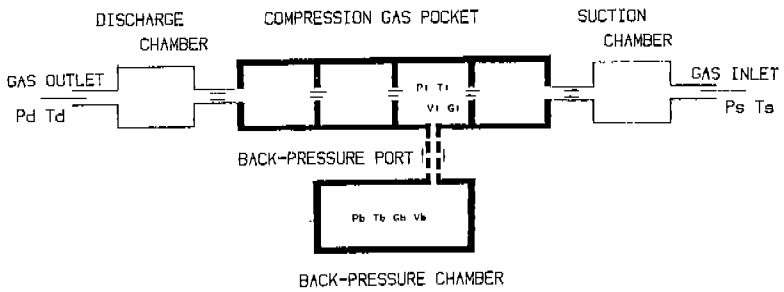


Figure 7 Analytical model of scroll compressor

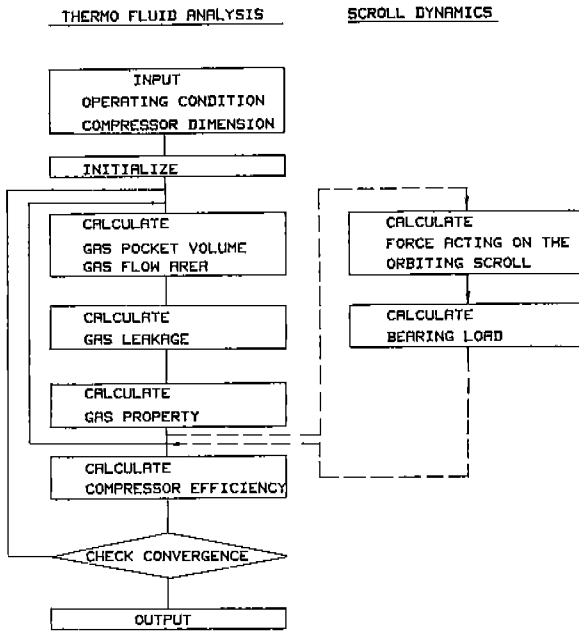


Figure 8 Flow diagram

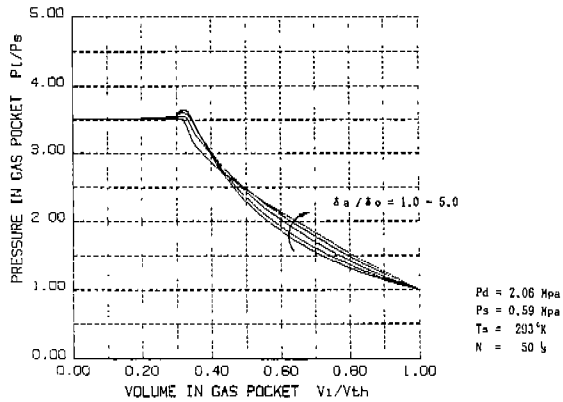


Figure 9 Effect of axial clearance on P-V diagram

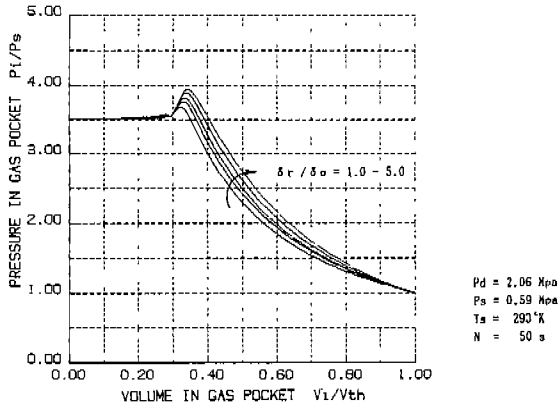


Figure 10 Effect of radial clearance on P-V diagram

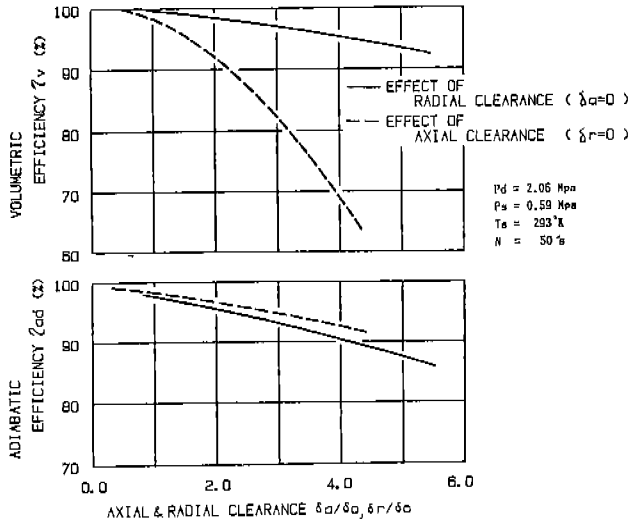


Figure 11 Effect of axial and radial clearances on compressor efficiency

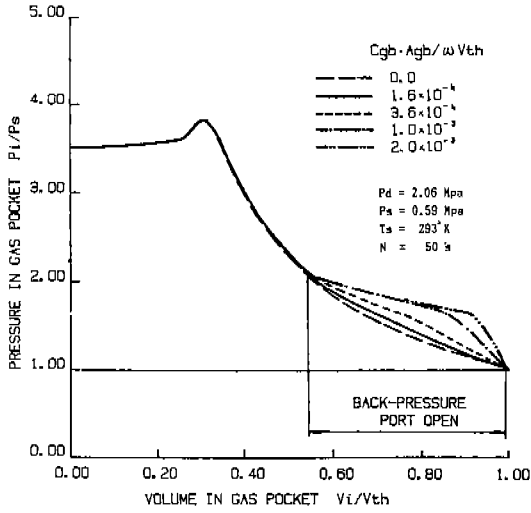


Figure 12 Influence of effective back-pressure port area on P-V diagram

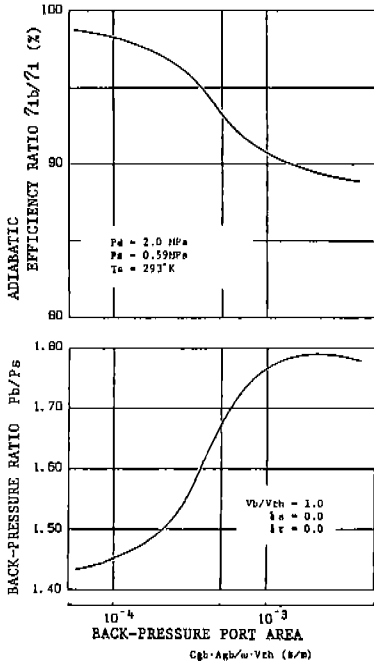


Figure 13 Variation of compressor efficiency and back-pressure with effective back-pressure port area